2 Formulation of the problem

The standards in force (GOST 32492-2015 Fiber-reinforced polymer bar for concrete reinforcement. Determination of physical-mechanical properties) recommend to use samples with reduced cross-section when performing an axial tension test aimed at determining the large diameter FRP-rebar strength properties. In the middle of the sample a kind of neck is made (Fig. 1, a) differing it from a standard sample (Fig. 1, b). Hence, due to the nature of composite material, the manufacturing of samples becomes much more labor-intensive (and thus, more expensive), and the probability of undercutting the fiber, which makes the neck asymmetrical, grows dramatically. On the other hand, if using standard samples, a need appears to fill sockets of very big length and thickness (Fig. 2, a); otherwise, the sample collapses due to the cut-off of the winding (Fig. 2, b) or due to the collapse of the socket itself, which in both cases results in a failure to determine the strength properties.

a)

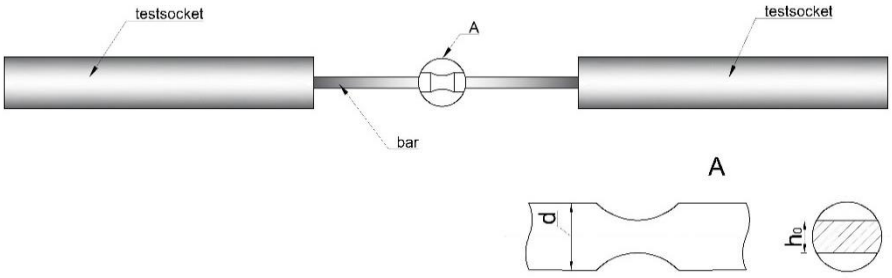

b)

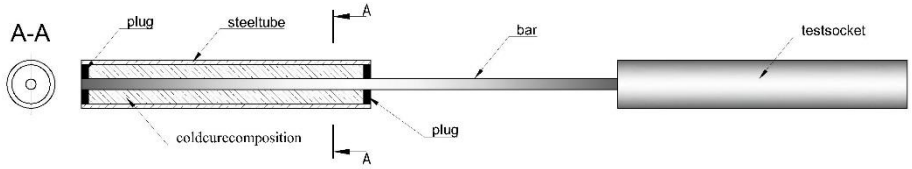

Fig. 1. FRP-rebar sample types used in the axial tension tests: a) sample with a flat neck; b) standard test sample.

Together with determining strength properties based on GOST 31938-2012 «Polymer composite reinforcement bars for reinforcing concrete structures. General specifications» it is necessary to experimentally identify the mass fractions of composite components. In particular, the FRP-rebar shall contain continuous reinforcement filler with a mass fraction of not less than 75%. These experiments only require availability of specialized equipment and are not technically complicated. However, the obtained values of the composite components' mass fractions can be used for the prediction mechanical properties of the material.

Thus, the task of this research is prediction the elastic and mechanical strength properties of large diameter FRP-rebar using additional experimental information (determination of mass fractions of components) and finite-element simulation.

a) b)

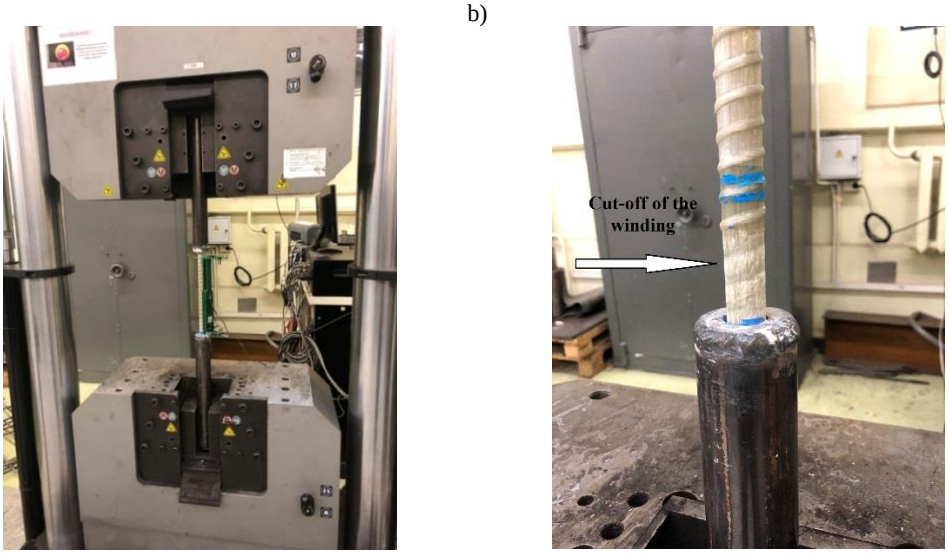

Fig. 2. Testing samples of large diameter composite rebar: a) the sample general view; b) the sample collapse due to the cut-off of the winding.

3 Experimental studies

The experiments were carried out on the basis of 8 mm diameter rebar (full program) and 18 mm diameter rebar (reduced program). The results of the 8 mm diameter rebar tests were later taken as a reference for the finite-element model verification. The plan of the experiment is shown in Table 2.

Table 2. Plan of the experiment.

Property	Diameter of rebar	
	8 mm	18 mm
Nominal diameter	+	+
Mass fraction of fiber	+	+
Tensile strength	+	–
Elastic modulus	+	+

Experiments were carried out in the Mechanical Laboratory named after prof. N.A. Belelubsky, Emperor Alexander I St. Petersburg State Transport University, according to GOST 31938-2012 and 32492-2015. The results of the experiment are shown in the Table 3.

Table 3. Results of the experiment.

Property	Unit of measurement	Standard, not less than	Diameter of rebar	
			8 mm	18 mm
Nominal diameter	mm	–	8.26	18.52
Mass fraction of fiber	%	75	79.80	81.96
Tensile strength	MPa	800	943	–
Elastic modulus	GPa	50	50.85	52.40

4 Analytical evaluations

Due to the unidirectional kind of rebar fiber reinforcement the initial calculation of the fiber composite elastic modulus was performed by mixture rule. For the composite material the upper (Voigt (1) [2]) and the lower (Reuss (2) [3]) Hill estimators of the FRP-rebar elastic modulus were obtained

$$E = \frac{V_a}{V_a + V_m} E_a + \frac{V_m}{V_a + V_m} E_m \tag{1}$$

$$\frac{1}{E} = \frac{V_a}{V_a + V_m} \frac{1}{E_a} + \frac{V_{\mathrm{M}}}{V_a + V_m} \frac{1}{E_m} \tag{2}$$

where V_m, E_m are the volume and the elastic modulus of the matrix (thermosetting resin),
V_a, E_a are the volume and the elastic modulus of the reinforcing filler (glass fiber).

Equations (1) and (2) can be presented through the volume fractions of the composite components

$$E = \tilde{V}_a \cdot E_a + \tilde{V}_m \cdot E_m \tag{3}$$

$$\frac{1}{E} = \tilde{V}_a \cdot \frac{1}{E_a} + \tilde{V}_m \cdot \frac{1}{E_m} \tag{4}$$

The volume fraction of the reinforcing glass fiber in the composite material is determined by formula

$$\tilde{V}_a = \frac{V_a}{V} = \frac{\tilde{C}_a \cdot \rho_m}{\tilde{C}_a \cdot \rho_m + \tilde{C}_m \cdot \rho_a} \tag{5}$$

where V is the total volume of composite,
$\tilde{C}_a$, $\tilde{C}_m$ are glass fiber and matrix mass fractions in the composite (respectively),
ρ_a, ρ_m are the values of glass fiber and matrix density (respectively).

In calculations we applied the values of composite components' properties provided by the FRP-rebar manufacturers. These are given in Table 4 [4].

Table 4. General mechanical properties of two types of glass fiber and PET.

Property	Units of measurement	Type of glass fiber		PET
		E	S	
Density	g/cm^3	2.54	2.40 to 2.58	1.38 to 1.40
Pristine fiber strength	MPa	3500	4600 to 4900	–
Elastic modulus	GPa	73	82 to 93	2.5 to 3
Resin tensile strength	MPa	–	–	40 to 140
Elongation at break	%	4.8	5.4	2 to 4

Thus, in calculations we assumed that $E_{\mathrm{A}} = 73$ GPa and $E_{\mathrm{M}} = 3$ GPa. The upper and lower boundaries of the elastic modulus obtained for FRP-rebar by equations (1) and (2) are shown in the diagrams depending on the volume of reinforcing filler (Fig. 3).

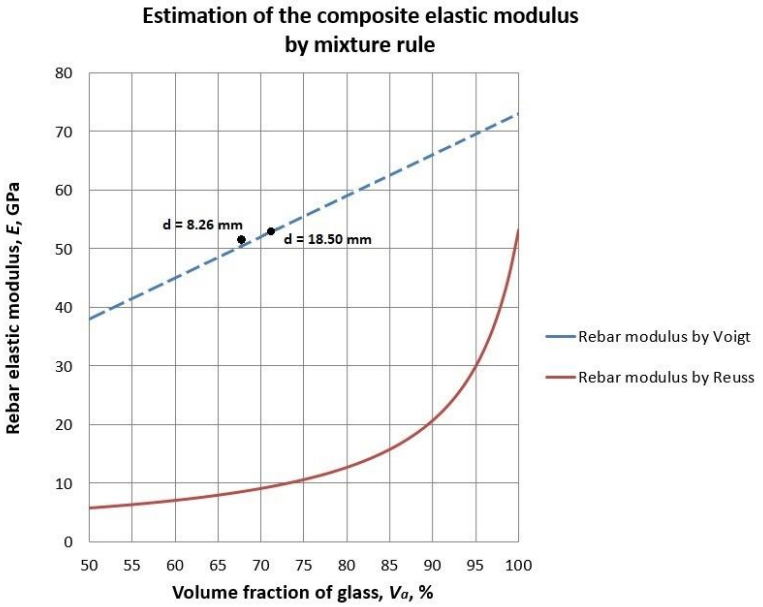

Fig. 3. Diagram showing the ratio of the composite elastic modulus and the volume fraction of the reinforcing material.

Points in the diagram (Fig. 3) show the values of the elastic modulus obtained experimentally for bars of 8.26 mm and 18.50 mm nominal diameter accounting for the exact values of reinforcing fiber volume fractions (67.8% and 70.9% respectively). Thus, it is proved that the use of the upper bound estimation of the elastic modulus (Voigt formula (1)) correlate well with the experimental data.

Similar equations for calculating the upper and lower boundaries of tensile strength by mixture rule are as follows

$$\sigma = \tilde{V}_a \cdot \sigma_a + \tilde{V}_m \cdot \sigma_m \tag{6}$$

$$\frac{1}{\sigma} = \tilde{V}_a \cdot \frac{1}{\sigma_a} + \tilde{V}_m \cdot \frac{1}{\sigma_m} \tag{7}$$

The results of the calculation (with respect to the input data given in Table 4) are shown in Fig. 4.

Once the results of experimental and analytical studies were compared, a significant difference was detected between the values obtained. As far as some analogous experimental data are concerned (source, https://www.owenscorning.com/composites), one can notice that the application of linear approximations, which are similar to those used for estimating the upper bound of the fiber composite elastic modulus (1), leads to a critical departure of the analytical values of limit stress (short-term tensile strength) from the experimental data. The actual FRP-rebar static strength appears to be lower than the estimators calculated by mixture rule (6). The reasons for this rest on a number of factors associated with non-homogeneity and multiple stages of the FRP-rebar fracture process as well as with the peculiarities of its manufacturing technology. Among these reasons are the following: action of the fiber initial stress that appears in the manufacturing process when the composite is cooling down due to the difference between the fiber and the matrix coefficients of thermal expansion; development of microcracks on the fiber surface; statistic variety of the fiber geometrical parameters resulting (in case of their abundance) in a

reduction of strength (the weakest-link model used for estimating reliability) and in a scale factor effect; clustering of collapse areas caused by the fact that FRP-rebar is initially manufactured by banding fiber in a strand; non-homogeneity of stress fields in undamaged fiber resulting from the collapse of the matrix and/or separate fibers.

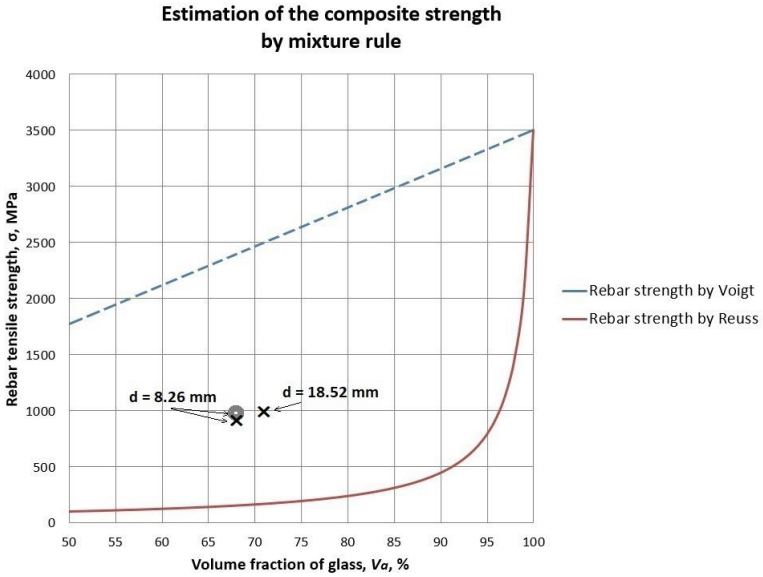

Fig. 4. Diagram showing the ratio of the composite tensile strength and the volume fraction of reinforcing material (**O** – experimentally; **X** – by means of finite-element simulation).

A fiber breakout causes a local increase in stress in the adjacent fibers as well as the fracture of the matrix in the proximity of breakout, and a failure of the interface links between strands, which leads to a reduction of the FRP-rebar total strength. In this case the topology of the elements parallel connection gets broken, and the linear relationship (6) based on the idea of the composite components' parallel connection doesn't allow for the description of the FRP-rebar tensile strength dependency on the glass fiber volume fraction.

The abovementioned microstructural features of the FRP-rebar collapse process can be directly accounted for in the strength estimation by means of forward mathematical simulation based on the multiple-option computational experiments using finite-element solutions.

5 Finite-element simulation

To predict the rebar tensile strength the stress-strain behavior of a representative volume of FRP-rebar was analyzed. Determination of the effective elastic moduli was performed on the basis of the finite-element homogenization method [5, 6]. In computational experiments the finite-element software ANSYS v.19.2 was used. The finite-element model of the representative elementary volume element for FRP-rebar accounts for the individual geometries of all fibers. In the finite-element model we used SOLID 185 3D hexagonal isoparametric finite elements based on the finite quadratic approximations of the displacement fields. Two 3D finite-element models of different single profile sections of the rebar (length: 15 mm) is shown in Fig. 5, and its properties are given in Table 5. The

volumetric content of the isotropic component shares presented in the models meets the experimental requirements.

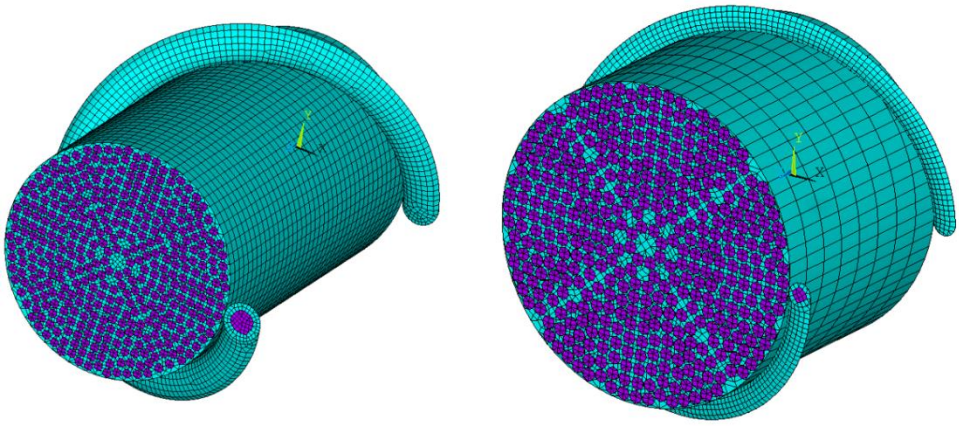

Fig. 5. FRP-rebar finite-element models.

Table 5. Parameters of finite-element model and solution.

Nominal diameter, mm	8.26	18.5
Number of nodes	201453	168036
Number of elements	401423	98601
Number of degrees of freedom	604359	504108
Method of solving the contact problem	MPC algorithm	

In the simulation kinematic boundary conditions were applied in the plane of symmetry (plane of endface clamping) and also static boundary conditions were applied to the front face (axial tension force). As a result we can see two different reactions of two samples after applying the same force. The value of the matching averaged component of the stress tensor for fiber for the sample with less diameter is higher than the value of the big one, Fig. 6.

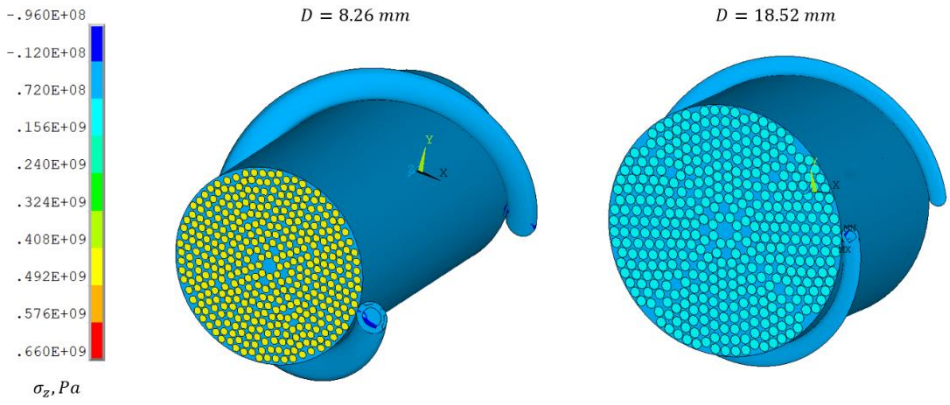

Fig. 6. Distribution of the tensile stress component in two models.

Analysis of the FRP-rebar failure process was based on the local strength approach that implied comparison of extremal values of stress-strain state characteristics of individual composite components with their strength parameters. It was assumed that mechanisms of each component fracture were of brittle type, so, as a criterion of fracture we took the condition when the maximum principal value of the stress tensor reached the value of tensile strength (see Table 4) of the corresponding composite component.

Comparison of the finite-element simulation results with the results of the experimental data (Fig. 4 and 5) proved a high level of correlation for the FRP-rebar 8.26 mm diameter sample and helped to forecast tensile strength for the FRP-rebar 18.52 mm diameter sample.

6 Conclusions

1. If direct tests are impossible, one can use formula (1) (the upper bound of the composite elastic modulus by Voigt) in order to determine the initial elastic modulus of large diameter FRP-rebar samples. However, it is necessary to carry out preliminary experiments and determine the volume fractions of composite components.

2. In the analysis of limit stress, linear approximation (6) applied for the purpose of estimating the fiber composite elastic modulus (1) leads to a significant departure from experimental data caused by the fact that many factors are not accounted for, especially those associated with non-homogeneity and multiple stages of the FRP-rebar collapse process as well as with the peculiarities of its manufacturing technology.

3. An algorithm is proposed to identify FRP-rebar tensile strength based on the experimental determination of the composite components' volume fractions and on the forward mathematical simulation of the collapse process of representative volume of FRP-rebar accounting for the microstructure, the initial technological micro-stress, and the analysis of the fiber breakout process evolution based on the finite-element method.

References

1. A. Benin, G. Bogdanova, S. Semenov, Appl Mech Mater, **617**, 215 (2014)
2. A. Reuss, Z. Angew. Math. und Mech, **9(1)**, 49 (1929)
3. W. Voigt, *Lehrbuch der Kristallphysik* (Teubner, Berlin, 1928)
4. A.V. Shirko, A.V. Spiglazov, A.N. Kamlyuk, A.S. Drobysh, J. Eng. Phys. Thermophys, **90(3)**, 705 (2017)
5. V. I. Gorbachev, Moscow Univ. Mech. Bull., **71(6)**, 137 (2016)
6. V. I. Gorbachev, A. N. Emel'yanov, Mech Sol, **49**, 73 (2014)